Photoactive Self-Standing Films Made of Layered Double Hydroxides with Arranged Porphyrin Molecules

ARTICLE *in* THE JOURNAL OF PHYSICAL CHEMISTRY C · OCTOBER 2011

Impact Factor: 4.77 · DOI: 10.1021/jp207505n

6 AUTHORS, INCLUDING:

Jan Demel
Academy of Sciences of the Czech Republic
24 PUBLICATIONS **356** CITATIONS
SEE PROFILE

Pavel Kubát
Academy of Sciences of the Czech Republic
164 PUBLICATIONS **1,940** CITATIONS
SEE PROFILE

Kamil Lang
Academy of Sciences of the Czech Republic
137 PUBLICATIONS **2,475** CITATIONS
SEE PROFILE

THE JOURNAL OF PHYSICAL CHEMISTRY C

ARTICLE

pubs.acs.org/JPCC

Photoactive Self-Standing Films Made of Layered Double Hydroxides with Arranged Porphyrin Molecules

Marie Jiřičková,[†] Jan Demel,[‡] Pavel Kubát,[§] Jiří Hostomský,[‡] František Kovanda,[†] and Kamil Lang*[,‡]

[†]Institute of Chemical Technology, Prague, Technická 5, 166 28 Praha, Czech Republic

[‡]Institute of Inorganic Chemistry of the AS CR, v.v.i., Husinec-Řež 1001, 250 68 Řež, Czech Republic

[§]J. Heyrovský Institute of Physical Chemistry of the AS CR, v.v.i., Dolejškova 3, 182 23 Praha 8, Czech Republic

Supporting Information

ABSTRACT: Transparent films of layered double hydroxides (LDH) have been prepared by the deposition of their chloroform dispersions. The advantage of this method is the potential to obtain large and transparent self-standing films, composed of highly ordered LDH platelets, with durability that allows further modifications by anion exchange. The LDH interlayer can be filled with anionic porphyrins that impose interesting photophysical and photochemical properties on the films. Intercalated porphyrins, 5,10,15,20-tetrakis(4-sulfonatophenyl)porphyrin (TPPS) and its palladium complex (PdTPPS), exhibit luminescence emission. The triplet state dynamics in the absence of oxygen are not affected by the LDH matrix, whereas the interaction of the triplet states with oxygen to produce singlet oxygen, $O_2(^1\Delta_g)$, is less effective in the film than in solution. High local concentrations of $O_2(^1\Delta_g)$ and of the triplet states within the films induce singlet oxygen-sensitized delayed fluorescence (SODF). This work is the first report on LDH-based materials capable of emitting SODF. The detailed kinetic analysis of SODF behavior indicates a short singlet oxygen lifetime of ~0.3 μs, probably due to the close proximity of hydroxide groups at the LDH layers.

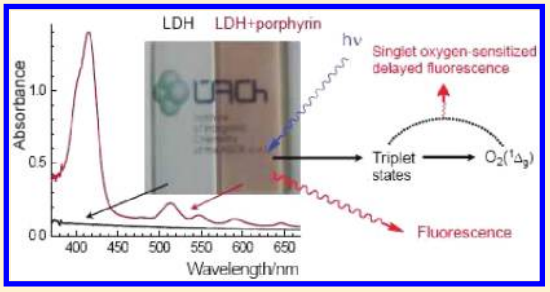

INTRODUCTION

Materials with arranged functional molecules that keep the inherent properties of individual molecules intact or that can change them as desired by matrix synergistic effects are of great interest.[1,2] A promising approach is based on self-assembly of functional molecules within a material, often inorganic, rather than on an approach where functional molecules are attached to the material surface by strong covalent bonding. This goal might be achievable using a 2D structure of layered double hydroxide (LDH) hosts with a flexible interlayer space.[3,4] The chemical composition of LDH can be described by the general formula $[M^{II}_{1-x}\ M^{III}_{x}(OH)_2]^{x+}[A^{m-}_{x/m}]^{x-}\cdot nH_2O$, abbreviated hereafter as $M^{II}_RM^{III}$—A, where M^{II} and M^{III} are divalent and trivalent metal cations within the hydroxide layers, A^{m-} is interlayer anion of valence m, and R is the M^{II}/M^{III} molar ratio ($R = (1-x)/x$). The open lamellar structure and the possibility of tuning the charge density of the hydroxide layers using their metal composition allow for the incorporation of functional inorganic and organic anions, often with control over their distribution and orientation in the interlayer space. For many practical applications where layered hydroxides serve as molecular scaffolds, carriers, or precursors (e.g., of related oxides), the hydroxide platelets could be aligned into well-defined continuous films. The transparent films, built from parallel hydroxide platelets, enable the direct utilization of the optical, photophysical, or photochemical functionalities of the imbedded molecules initiated by an external light source.

LDH-based films can be prepared by in situ growth and physical deposition methods.[5] Deposition methods are relatively easy to perform using LDH of an appropriate composition, either as a powder or as separated hydroxide layers obtained by LDH delamination. As-prepared LDH powders are polydisperse materials, and the deposition of their suspensions on a solid support generally leads to fragile films of low transparency due to the random orientation of the hydroxide platelets.[6] These problems can be overcome using dispersions with a narrow crystallite size distribution and a higher aspect ratio that favors face-to-face and edge-to-edge interactions between individual platelets.[7] The uniform, small size of hydroxide platelets (lateral size ~40 nm) results in a uniform LDH film. These films, containing fluorescent molecules with interesting photophysical properties,[8,9] are well-suited for the fabrication of transparent and self-standing films that can be peeled off a support.[10] The latter approach is based on manipulations with nanoscopic hydroxide layers obtained by LDH delamination: restacking into thin transparent films or self-standing films,[11] mixing with functional molecules (organic or inorganic simple molecules, polymers) to build layer-by-layer assemblies with properties that are tuned by the nature of functional molecules,[5,12] mixing hydroxide layers of varying cation compositions or charges,[13−15] or combining with

Received: August 5, 2011
Revised: September 21, 2011
Published: September 22, 2011

carbon nanotubes and nanosheets.[16] The films, especially well-oriented ones, can be suitable components for optical, electrical, and magnetic devices, sensors, or can be used as nanoreactors.[5,12]

Several groups described the intercalation of porphyrins and related phthalocyanines bearing anionic groups into LDH and layered zinc hydroxide salts inspired by catalytic[17−20] and photophysical[21−23] properties of these materials. Porphyrins and related macrocycles are effective photosensitizers with the ability to produce singlet oxygen, $O_2(^1\Delta_g)$.[24] The photosensitized production of $O_2(^1\Delta_g)$ is based on excitation of a photosensitizer to the triplet states, followed by energy transfer to the ground electronic state of oxygen that is excited to the lowest singlet state, $O_2(^1\Delta_g)$. It has been reported that porphyrins also act as photosensitizers after their intercalation between hydroxide layers.[21−23] This photoactivity was also described for LDH films prepared from delaminated LDH in formamide.[25] However, these films were thin and fragile, and the attempts to obtain thicker films ended with film disintegration during the formamide evaporation.

In this work, we combine porphyrins having high $O_2(^1\Delta_g)$ quantum yields with the ability of Mg_2Al LDH hosts to intercalate anionic porphyrins and act as well-defined and stable carriers. We report on a simple method for preparing self-standing LDH/porphyrin hybrid films based on the ability of LDH with intercalated dodecyl sulfate anions to be well-dispersed in chloroform, forming suspensions that are well-suited for the preparation of large-area and transparent self-standing films. In addition, the films have high stability in water and high affinity toward anionic porphyrins that allow for the fabrication of photoactive films whose photoactivity can be tuned by the amount of intercalated porphyrin molecules.

EXPERIMENTAL METHODS

Materials. The dihydrochloride of 5,10,15,20-tetrakis(4-sulfonatophenyl)porphyrin, TPPS, tetrasodium salt of Pd(II)-5,10,15,20-tetrakis(4-sulfonatophenyl)porphyrin, PdTPPS, (both Frontier Scientific Europe), $Mg(NO_3)_2\cdot 6H_2O$, $Al(NO_3)_3\cdot 9H_2O$, NaOH, $CHCl_3$, ethanol (all Penta), and sodium dodecyl sulfate (Sigma Aldrich) were used as purchased. Quartz glass plates were washed by a mixture of H_2SO_4 and H_2O_2 (3:1) prior to layer deposition.

Synthesis of Mg_2Al-DS. LDH with a Mg/Al molar ratio of 2 and with intercalated dodecyl sulfate anions (DS), abbreviated hereafter as Mg_2Al-DS, was prepared by coprecipitation under nitrogen as follows: 34.66 g of sodium dodecyl sulfate (0.12 mol, 100% excess related to the anion exchange capacity) was dissolved in 300 mL of carbonate-free distilled water. The solution was placed into a stirred batch reactor and heated to 80 °C. An aqueous solution (300 mL) of $Mg(NO_3)_2$ and $Al(NO_3)_3$ ($c_{(Mg+Al)}$ = 1.0 mol L^{-1}, Mg/Al molar ratio = 2) was added with a flow rate of 5.0 mL min^{-1}. The flow rate of simultaneously added NaOH (1 mol L^{-1}) was controlled to maintain the reaction pH value of 10.0 ± 0.1. Coprecipitation was carried out under vigorous stirring at 80 °C. The resulting suspension was stirred at 80 °C for 24 h, followed by filtration and thorough washing with water and ethanol. The obtained product was dried at 60 °C on air. The elemental and thermogravimetric analyses confirmed the chemical composition $Mg_{2.1}Al(OH)_{6.2}(DS)\cdot 2H_2O$. (See the Supporting Information for more details.)

Preparation of the Mg_2Al-DS Films. The Mg_2Al-DS powder (125 mg) was shaken in 5 mL of chloroform for 24 h at room temperature. The films prepared by casting of a suspension immediately after the shaking exhibited high roughness and low transparency. Therefore, the suspension was allowed to settle for 1 h, during which time larger LDH particles concentrated at the interface. Dispersion below the interface was carefully taken, cast on quartz plates (0.1 mL cm^{-2}), and allowed to air-dry slowly. This procedure was repeated until the film weight was ∼4 mg cm^{-2} (7−10 cycles).

Preparation of the Mg_2Al-DS/Porphyrin Films. The Mg_2Al-DS films were inserted in 20 mL of TPPS or PdTPPS aqueous solution (10^{-4} mol L^{-1}, pH 7.0) and heated to 50 °C. The films with different amount of intercalated porphyrins were prepared by varying time of anion exchange treatment.

Preparation of the Self-Standing Films. The films were obtained by peeling from a quartz plate after a 30 min treatment in water at 50 °C.

Instrumental Methods. Powder X-ray diffraction (XRD) patterns were recorded on a PANalytical X'Pert PRO diffractometer equipped with a conventional X-ray tube (Co Kα radiation, 40 kV, 30 mA) and a multichannel detector X'Celerator with an antiscatter shield. Qualitative analysis was performed with the HighScorePlus software package (PANalytical, Almelo, The Netherlands, version 3.0) and the JCPDS PDF-2 database.[26] All measurements were performed in reflection mode. Scanning electron microscopy (SEM) images were collected using a Philips XL 30 CP at 25 kV. The Fourier-transform infrared spectra (FTIR) were collected on a Nicolet NEXUS 670 FT spectrometer using KBr pellets. The absorption spectra were recorded on a Perkin-Elmer Lambda 35 spectrometer equipped with a Labsphere RSA-PE-20 integration sphere in transmittance mode.

The steady-state (TPPS, PdTPPS, $O_2(^1\Delta_g)$) and time-resolved (TPPS) luminescence properties were monitored using a Fluorolog 3 spectrometer (Horiba Jobin Yvon) with the Mg_2Al-DS/TPPS and Mg_2Al-DS/PdTPPS films oriented at 30° to an excitation source. The steady-state emission spectra were recorded with a 450 W Xe lamp as an excitation source. In the case of the emission spectra of $O_2(^1\Delta_g)$, the fluorescence of TPPS and scattered light was eliminated using a Shott RG 830 glass filter, and the transmitted emission was detected using a Hamamatsu H10330-45 photomultiplier. Fluorescence lifetime measurements of TPPS were performed using a laser-diode excitation at 405 nm (NanoLED-405LH, pulse width 750 ps, repetition rate 1 MHz). The emission was recorded at both fluorescence maxima using a cooled TBX-05-C photon detection module in a time-correlated single-photon counting regime. The decay curves were fitted to exponential functions using the iterative reconvolution procedure of the DAS6 software (v. 6.4, Horiba Jobin Yvon, 2009).

The time-resolved near-infrared luminescence of $O_2(^1\Delta_g)$ at 1270 nm was monitored using a Ge detector upon laser excitation by a Lambda Physik Compex 102 excimer laser (λ_{exc} = 308 nm, pulse width 28 ns, incident energy 3.4 mJ/pulse). The short-lived signal produced by the scattering of an excitation laser pulse and by porphyrin fluorescence was eliminated by exciting the sample in vacuum and subtracting the obtained signal from the signal recorded in oxygen or air atmosphere. Nanosecond transient absorption (within 450−600 nm), singlet oxygen-sensitized delayed fluorescence (SODF), and PdTPPS luminescence experiments were performed with a Lambda Physik FL 3002 dye laser (425 nm, 0.5 - 2 mJ/pulse), and the corresponding signals were recorded on a laser kinetic spectrometer LKS 20 (Applied Photophysics). The signal-to-noise ratio was improved by averaging 100 to 500 individual traces.

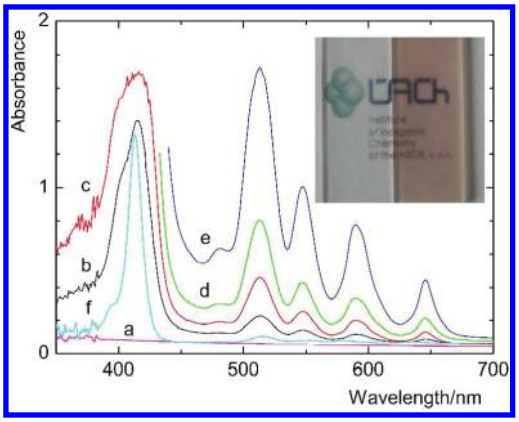

Figure 1. UV/vis absorption spectra of the Mg_2Al-DS/TPPS films deposited on a quartz slide after treatment with aqueous 10^{-4} M TPPS for 5 (b), 15 (c), 30 (d), and 180 min (e) at 50 °C compared with the original Mg_2Al-DS film (a) and a TPPS aqueous solution (f). Inset: Photographs of transparent Mg_2Al-DS (left, corresponds to absorption spectrum (a)) and Mg_2Al-DS/TPPS (right, corresponds to absorption spectrum (b)) films on quartz slides.

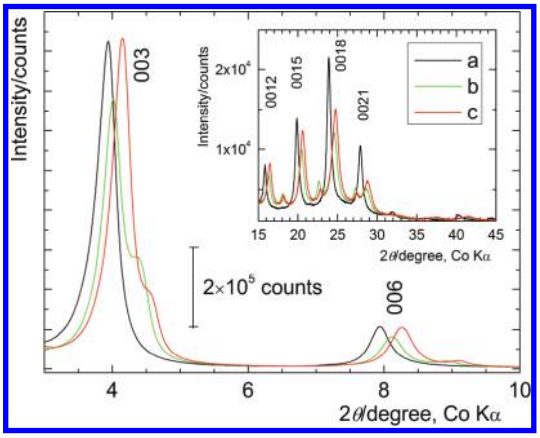

Figure 2. Powder XRD patterns of the films: Mg_2Al-DS (a), Mg_2Al-DS/TPPS (180 min treatment) (b), and Mg_2Al-DS/PdTPPS (120 min treatment) (c). Inset: Basal diffraction lines recorded at longer angles.

RESULTS AND DISCUSSION

Films. The Mg_2Al-DS sample was prepared by direct synthesis, with the identity confirmed by elemental analysis, FTIR, and XRD patterns that are in good agreement with the literature.[27] The transparent self-standing films of 10 to 20 μm in thickness were obtained from dispersions of Mg_2Al-DS in $CHCl_3$ (Figure 1a, inset). For comparison, self-standing films prepared using the acetate form of LDH in water were between 10 and 25 μm,[11] and the films prepared using separate nucleation and aging steps reached a thickness of ~24 μm.[28] The durability of our films allows anion exchange, producing self-standing photoactive films. However, the films become fragile when dried.

The XRD patterns of the films show a number of basal 00*l* diffraction lines (Figure 2), whereas the nonbasal diffractions around 40−45 and 71−74° disappear because of the preferential orientation of restacked platelets along a support surface. This finding is also confirmed by SEM (Figure 3). A basal spacing of 25.9 Å for the Mg_2Al-DS film, corresponding to the position of the d_{003} line, is fully comparable to a value of 26.0 Å for the original Mg_2Al-DS powder. The porphyrins, TPPS and PdTPPS, exchange for intercalated DS by treatment of the films in aqueous porphyrin solutions at 50 °C. This phenomenon is evidenced by the splitting of the basal diffraction lines into two separated lines, which is especially clear at larger angles (Figure 2, inset). The phase with a basal spacing around 25 Å is attributed to the original Mg_2Al-DS. A slightly tighter packing of the hydroxide layers can be ascribed to a rearrangement of DS molecules within the LDH interlayer. The phases with basal spacings of 22.9 and 22.5 Å for the Mg_2Al-DS/TPPS and Mg_2Al-DS/PdTPPS films, respectively, contain the corresponding porphyrins within the LDH interlayer. These phases are in good agreement with XRD results on the Mg_2Al LDH powders that contain intercalated TPPS and exhibit a basal spacing between 20.8 and 23.0 Å depending on the intercalation method, interlayer water content, and hydrothermal treatment.[21,22] The arrangement of porphyrin molecules in the interlayer space of LDH was described in detail for intercalated Zn-5,10,15,20-tetrakis(4-sulfonatophenyl)porphyrin.[22] In that case, the interlayer space is filled with disordered, nearly parallel porphyrin units with a dihedral angle between 0 and 10°. The distance between two neighboring central atoms varies from 6 to 9 Å. The porphyrin planes are not perpendicular to the hydroxide layers but slightly inclined with the average angle between the porphyrin plane and the layer normal of ~14°.

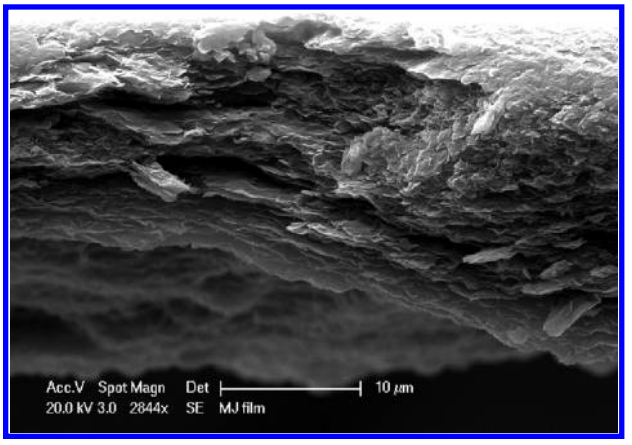

Figure 3. SEM image of the cross section of the Mg_2Al-DS self-standing film.

Absorption and Fluorescence Properties. The results presented above show that the Mg_2Al-DS films are suitable hosts for both TPPS and PdTPPS anions. The absorption spectra of the films can yield additional information because of their sensitivity to porphyrin aggregation.[29] The mutual arrangement of porphyrin units in stacked aggregates falls into one of two types: (i) J-aggregates (edge-to-edge), characterized by a red shift of the Soret band, or (ii) the formation of H-aggregates (face-to-face), accompanied by a blue shift of this band. The aggregation of porphyrins usually leads to a fast competitive relaxation of the excited states associated with a decrease in the quantum yields of fluorescence and the triplet states, thus decreasing the overall photoactivity of a material.

The progressive intercalation of TPPS is documented by the absorption spectra of the Mg_2Al-DS/TPPS films (Figure 1). Whereas the Mg_2Al-DS film is transparent (Figure 1a), the Mg_2Al-DS/TPPS films show a gradual increase in TPPS absorption with increasing duration of the exchange reaction. The absorption spectra are characterized by the Soret band at 416 nm and four Q-bands at 513, 547, 590, and 646 nm. We recall that the

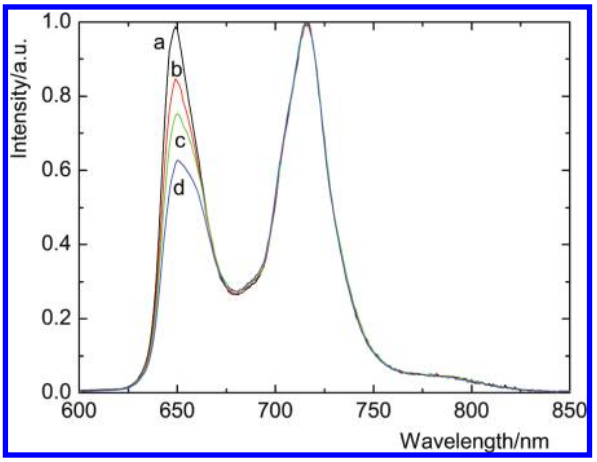

Figure 4. Normalized fluorescence emission spectra of the Mg_2Al-DS/TPPS films with varying amounts of intercalated TPPS: treatment with aqueous 10^{-4} M TPPS for 5 (a), 15 (b), 30 (c), and 180 min (d) at 50 °C. Excited at 514 nm.

J-aggregates of TPPS are formed upon protonation of the porphyrin units,[30] that is, under conditions that are excluded in the present case. The H-type stacking is connected with a large red shift of the fluorescence emission bands, which is not observed in our measurements (see below).[30] As shown in Figure 1, the intercalation of TPPS only broadens the Soret band in comparison with the sharp Soret band of the monomeric species in an aqueous solution and slightly red-shifts the Q-bands. These variations exclude the presence of the specific stacked structures of TPPS molecules within the LDH interlayer and can be interpreted in terms of a range of binding sites. The results are similar to those reported for powdered Mg_2Al-TPPS and Zn_RAl-TPPS (R = 2 or 4) samples previously described.[21,22,25] The absorption spectra of the Mg_2Al-DS/PdPPS films are similar to those of monomeric PdTPPS in aqueous solution (Figure S1 in the Supporting Information). The Soret band is only slightly broadened, and the Q(1,0) band is shifted by 3 nm to 523 nm. Similarly to TPPS, no specific aggregates of PdTPPS in the interlayer are expected.

Fluorescence emission spectra confirm the identity of intercalated porphyrins. In the case of TPPS, the Q(0,0) and Q(0,1) emission bands at 642 and 703 nm measured in aqueous solution are slightly shifted to 649 and 716 nm in the Mg_2Al-DS/TPPS films (Figure 4). Interestingly, the contribution of the Q(0,1) emission band increases at the expense of the Q(0,0) band with increasing loading of TPPS molecules. These changes correlate with the shortening of corresponding fluorescence lifetimes. The emission decays were in all cases best characterized by two lifetimes. The lifetimes shorten from 10.2 (82%) and 4.6 ns (18%) for the least exchanged film (5 min treatment) to 9.2 (84%) and 3.2 ns (16%) for the heavily exchanged film (180 min treatment). The fluorescence variations are probably related to subtle changes in the mutual orientation of TPPS molecules, the orientation of TPPS planes with respect to the LDH hydroxide layers, or both.

The emission spectra of PdTPPS in aqueous solution and in the interlayer space of LDH observed in air atmosphere differ in the intensity of the respective bands due to the limited quenching of the porphyrin triplet states by oxygen in the latter case. Whereas the fluorescence Q(0,1) band at 606 nm is much more intensive than phosphorescence bands at 700 and 765 nm in solution, the intensity ratio of phosphorescence/fluorescence is the opposite for intercalated PdTPPS, with the intensive phosphorescence bands (0,0) and (0,1) at 687 and 760 nm, respectively (Figure S2 in the Supporting Information).

Triplet States. The triplet states of porphyrin molecules in the LDH interlayer are produced by intersystem crossing from excited singlet states (eq 1) and deactivate spontaneously (eq 2) or via molecular oxygen (eqs 3 and 4).

$$^1\mathrm{TPPS}^* \xrightarrow{k_s} {}^3\mathrm{TPPS} \quad (1)$$

$$^3\mathrm{TPPS} \xrightarrow{k_{T0}(=1/\tau_{T0})} {}^1\mathrm{TPPS} \quad (2)$$

$$^3\mathrm{TPPS} + \mathrm{O}_2(^3\Sigma_g^-) \xrightarrow{k_q'} {}^1\mathrm{TPPS} + \mathrm{O}_2(^1\Delta_g) \quad (3)$$

$$^3\mathrm{TPPS} + \mathrm{O}_2(^3\Sigma_g^-) \xrightarrow{k_q''} {}^1\mathrm{TPPS} + \mathrm{O}_2(^3\Sigma_g^-) \quad (4)$$

Furthermore, a small portion of the triplet states reacts with $O_2(^1\Delta_g)$, repopulating the excited singlet states, ^{1}TPPS* (see below). We have already described the dynamics of the triplet states of intercalated TPPS in Mg_RAl LDH powders using time-resolved diffusion reflection spectroscopy.[21] In these samples, the triplet states exhibited biexponential behavior with both lifetimes decreasing from 7 and 68 μs in nitrogen to 4 and 50 μs in air.

In contrast with powders, the Mg_2Al-DS/TPPS films are transparent, and the triplet states of TPPS can be probed by transient absorption spectroscopy. Triplet state decays are monoexponential with lifetimes that are not affected by the porphyrin loading within the experimental error (Figure S3 in the Supporting Information). The triplet lifetime of TPPS in vacuum, τ_{T0}, is ~500 μs, and some uncertainty of this value is due to a low signal-to-noise ratio. Because the lifetimes in oxygen-free aqueous solutions are in the range of 290−510 μs,[24] this result shows that the LDH hydroxide layers do not interact with the triplet states in a measurable way and can be considered as an inert environment. The decay is accelerated by oxygen but to a lesser extent than in a solvent due to slower oxygen diffusion in the solid matrix.[25] To evaluate the overall quenching rate constant of the triplet states, k_q ($k_q = k_q' + k_q''$), we measured the decay curves at different oxygen pressures, p_{O_2}, and the corresponding triplet lifetimes, τ_T, were cast into the Stern−Volmer plot, $1/\tau_T = 1/\tau_{T0} + k_q p_{O2}$ (Figure S4 in the Supporting Information). The obtained k_q of 2.5 ± 0.1 $Pa^{-1}\,s^{-1}$ and the linear character of the plot within all studied pressures (up to 120 kPa) indicates that TPPS molecules are accessible to oxygen similarly to porphyrin molecules embedded in polymeric nanofibers.[31]

The dynamics of the triplet states of intercalated PdTPPS in the Mg_2Al-DS/PdTPPS films were probed by both time-resolved transient and time-resolved luminescence spectroscopies. Both methods give comparable results; however, time-resolved luminescence spectroscopy produces the data with a much better signal-to-noise ratio. Quenching of the triplet states is clearly documented by Figure 5, showing relaxation of PdTPPS phosphorescence at different oxygen pressures. The intensities plotted on the semilogarithmic scale exhibit an upward curvature, indicating that the deactivation of PdTPPS triplet states does not follow first-order kinetics. The deactivation may be well-fitted by the dispersed kinetics model of Albery et al.[32] with the Gaussian distribution of the logarithm of the triplet lifetimes to give the median triplet lifetime, $\tau_{T,median}$, and the width of the lifetime

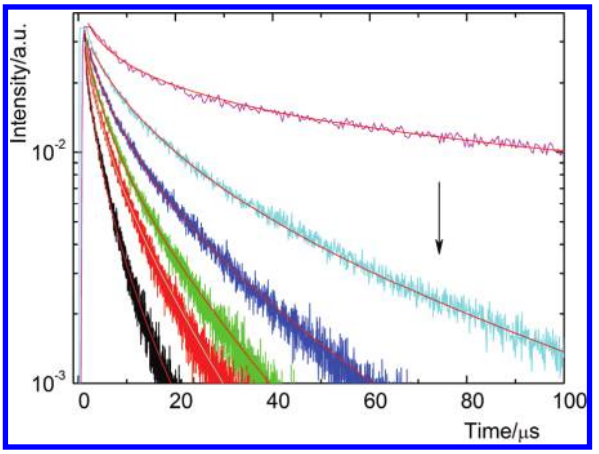

Figure 5. Relaxation of PdTPPS phosphorescence in the Mg_2Al-DS/PdTPPS film (5 min treatment) at different oxygen pressures (λ_{exc} = 425 nm, 0.5 mJ/pulse, recorded at 690 nm). The red curves are least-squares fits to the experimental curves based on Albery et al.[32] The arrow shows increasing O_2 pressure (vacuum, 100, 210, 300, 400, 760 Torr).

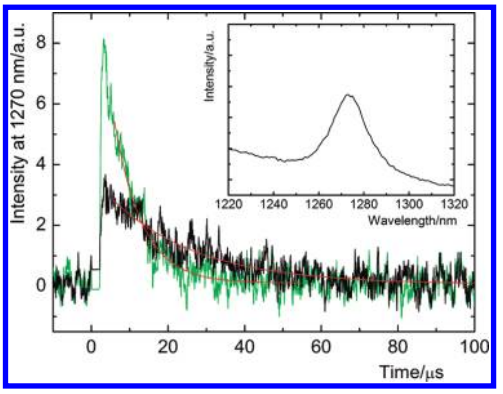

Figure 6. Time dependencies of the $O_2(^1\Delta_g)$ luminescence signals in air (black line) and oxygen (green line) atmosphere after the excitation of TPPS in the Mg_2Al-DS/TPPS film (180 min treatment). The red lines are least-squares monoexponential fits. Inset: Emission band of $O_2(^1\Delta_g)$ upon excitation of the film at 515 nm on air.

distribution, γ. The logarithm of triplet lifetimes is normally distributed with a standard deviation $\gamma^{1/2}$. Therefore, 68% of the triplet states exhibit the lifetime within the interval $\tau_{T,median}\exp(-\gamma^{1/2})$ and $\tau_{T,median}\exp(\gamma^{1/2})$ and 95% within the interval $\tau_{T,median}\exp(-\gamma)$ and $\tau_{T,median}\exp(\gamma)$. (See the Supporting Information for more details.) The corresponding fits are presented in Figure 5 with a shared value γ of 1.6. This value indicates a broad distribution of the triplet lifetimes (95% within $\tau_{T,median}/5$ and $5\tau_{T,median}$), thus reflecting the high heterogeneity of PdTPPS triplet states in the LDH interlayer. In the absence of oxygen (in vacuum), the role of matrix heterogeneity is substantially greater; that is, γ is 5.5. The Stern–Volmer plot for $\tau_{T,mean}$ in the presence of oxygen yields a rate constant k_q of 4.3 s^{-1} Pa^{-1}, where mean lifetime, $\tau_{T,mean}$, is defined as the expected value τ_T ($\tau_{T,mean} = \int_0^\infty f(\tau_T)\,\tau_T\,d\tau_T = \tau_{T,median}\exp(\gamma^2/4)$; see the Supporting Information). On the basis of these results, the kinetic heterogeneity of the PdTPPS triplet states is higher than that of intercalated TPPS.

Singlet Oxygen Formation. The formation of $O_2(^1\Delta_g)$ in the films is indicated by the quenching of the triplet states by oxygen.

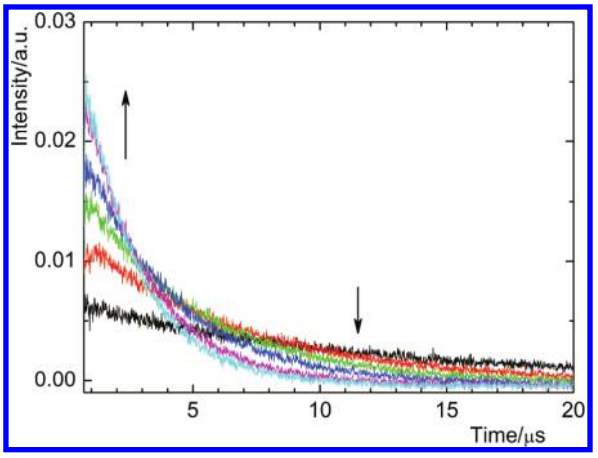

Figure 7. Kinetics of SODF at different oxygen pressures after excitation of TPPS in the Mg_2Al-DS/TPPS film (30 min treatment) (λ_{exc} = 425 nm, 0.5 mJ/pulse, recorded at 650 nm). The arrows show changes with increasing pressure of O_2 from 100 to 760 Torr (100, 200, 300, 400, 600, 760 Torr).

However, the direct evidence is the presence of an emission band at 1273 nm, which is characteristic of $O_2(^1\Delta_g)$ (Figure 6, Figure S5 in the Supporting Information). Emission at this wavelength decays monoexponentially with an apparent $O_2(^1\Delta_g)$ lifetime of 7 and ~20 μs in oxygen and air, respectively (Figure 6). The fact that the decay is affected by oxygen pressure implies that it is controlled by the decay of the parental triplet states. Therefore, the intrafilm lifetime of $O_2(^1\Delta_g)$ ($\tau_\Delta = 1/k_O^1$, eq 5) is short probably due to interaction with interlayer water, the surrounding LDH matrix, or both.

$$O_2(^1\Delta_g) \xrightarrow{k_O^1} O_2(^3\Sigma_g^-) \qquad (5)$$

Singlet Oxygen-Sensitized Delayed Fluorescence (SODF). We have shown that 5,10,15,20-tetraphenylporphyrin (TPP) embedded in polymeric nanofibers produces delayed fluorescence at a porphyrin fluorescence wavelength of 650 nm.[31,33] The repopulation of the excited singlet states, ^{1}TPP*, proceeds via the reaction of the triplet states ^{3}TPP with $O_2(^1\Delta_g)$ (eq 6).

$$^3\mathrm{TPP} + O_2(^1\Delta_g) \xrightarrow{k_q^1} {}^1\mathrm{TPP}^* + O_2(^3\Sigma_g^-) \qquad (6)$$

SODF becomes important in solids with concentrated immobilized triplets and relatively high oxygen mobility.[31,33,34] This is evidently the case for the Mg_2Al-DS/TPPS films that exhibit SODF within the microsecond time window with the intensity strongly affected by oxygen (Figure 7). The kinetic analysis of a set of SODF decay curves obtained at different oxygen pressures was performed using a previously applied homogeneous model, where $O_2(^1\Delta_g)$ is removed from the reaction system by the repopulation reaction (one channel leads to ^{1}TPPS*, eq 6) and by monomolecular decay (eq 5).[31] The triplet lifetimes were obtained by independent measurements with the same samples. Therefore, only two kinetic parameters, common for the whole set of measurements (i.e., for all SODF decay curves at different oxygen pressures), are evaluated: the lifetime τ_Δ and the product $k_q^1[^3\mathrm{TPPS}]_0$, where k_q^1 is the rate constant of the repopulation reaction (eq 6) and $[^3\mathrm{TPPS}]_0$ is the initial concentration of the triplet states. (The concentration of triplet states at time t follows

the relationship $[^3\text{TPPS}] = [^3\text{TPPS}]_0 \exp(-t/\tau_T)$.) The equation used in fitting is as follows

$$I_{SODF} = A_{SODF} y^{b+1} e^{ay} \int_y^1 e^{-aw} w^{-b}\, dw \quad (7)$$

where w is the dimensionless time variable, $y = \exp(-t/\tau_T)$, parameter a is $a = k_q^1[^3\text{TPPS}]_0\, \tau_T$, parameter b is $b = k_O^1\, \tau_T = \tau_T/\tau_\Delta$, and A_{SODF} is a scale constant. Accordingly, a singlet oxygen lifetime, τ_Δ, is 0.3 ± 0.1 μs, and $k_q^1[^3\text{TPPS}]_0 \leq 1\ \mu s^{-1}$. The results of kinetic analysis (see the Supporting Information for more details) indicate that the major part of $O_2(^1\Delta_g)$ decomposes via monomolecular decay (eq 5); nevertheless, the repopulation reaction (eq 6) is an important channel of the $O_2(^1\Delta_g)$ decay as a part of the SODF mechanism.

The evaluated singlet oxygen lifetime is very short. The lifetime is even shorter than that in water ($\tau_\Delta \approx 3.5\ \mu s$)[35] and points to the key role of the LDH matrix in the fate of $O_2(^1\Delta_g)$. Because the hydroxide groups are effective quenchers of $O_2(^1\Delta_g)$,[35] we propose that the hydroxide layers composed of the octahedral framework of the hydroxide groups with a possible contribution of interlayer water are responsible for deactivation. To the best of our knowledge, this work gives the first estimation of the interstructural $O_2(^1\Delta_g)$ lifetime. It is not possible to compare the obtained results with the effects of other inorganic carriers. The reported lifetimes in zeolites or silica were obtained by the time-resolved near-infrared luminescence of $O_2(^1\Delta_g)$, but the lifetimes of the parent triplet states of sensitizers used were not considered.[36−38] An upper limit of the $O_2(^1\Delta_g)$ lifetime in the interior of the supercages of zeolite Y was determined by the analysis of the photo-oxygenation kinetics of the products, yielding a value of 7.5 μs.[39]

CONCLUSIONS

We report on the simple fabrication of transparent, self-standing LDH films with photophysical properties that are tuned by intercalated anionic porphyrins, TPPS and PdTPPS. Porphyrin molecules are fixed in the interlayer and do not interact with each other in either ground or triplet states. Oxygen diffusion in the films, although limited when compared with that in solutions, allows energy transfer between porphyrin triplet states and ground-state oxygen to form $O_2(^1\Delta_g)$. The proximity of the porphyrin triplet states and their interaction with $O_2(^1\Delta_g)$ contributes to the repopulation of the fluorescent excited singlet states of TPPS. For practical applications of the films as sensors or carriers of photoactive molecules to possible biological targets, further study of their sensitivity, accuracy, and long-term stability in appropriate environments will be necessary.

ASSOCIATED CONTENT

Supporting Information. Details of the elemental analysis, analysis of PdTPPS phosphorescence in the Mg_2Al-DS/PdTPPS films, analysis of SODF, absorption spectra, luminescence spectra, and TPPS triplet states. This material is available free of charge via the Internet at http://pubs.acs.org.

AUTHOR INFORMATION

Corresponding Author
*E-mail: lang@iic.cas.cz.

ACKNOWLEDGMENT

This work was supported by the Czech Science Foundation (P207/10/1447) and by the Ministry of Education, Youth and Sports of the Czech Republic (MSM 6046137302). We are grateful to Petr Bezdička (IIC, ASCR, Řež) for the XRD measurements.

REFERENCES

(1) Takagi, S.; Eguchi, M.; Tryk, D. A.; Inoue, H. *J. Photochem. Photobiol., C* **2006**, *7*, 104–126.
(2) Sanchez, C.; Julián, B.; Belleville, P.; Popall, M. *J. Mater. Chem.* **2005**, *15*, 3559–3592.
(3) Evans, D. G.; Slade, R. C. T. In *Layered Double Hydroxides (Structure and Bonding)*; Duan, X., Evans, D. G., Eds.; Springer-Verlag: Berlin, 2006; Vol. 119, pp 1−87.
(4) Leroux, F.; Taviot-Guého, C. *J. Mater. Chem.* **2005**, *15*, 3628–3642.
(5) Guo, X.; Zhang, F.; Evans, D. G.; Duan, X. *Chem. Commun.* **2010**, *46*, 5197–5210.
(6) Gardner, E.; Huntoon, K. M.; Pinnavaia, T. J. *Adv. Mater.* **2001**, *13*, 1263–1266.
(7) Zhao, Y.; Li, F.; Zhang, R.; Evans, D. G.; Duan, X. *Chem. Mater.* **2002**, *14*, 4286–4291.
(8) Shi, W.; Wei, M.; Lu, J.; Li, F.; He, J.; Evans, D. G.; Duan, X. *J. Phys. Chem. C* **2008**, *112*, 19886–19895.
(9) Yan, D.; Lu, J.; Wei, M.; Evans, D. G.; Duan, X. *J. Phys. Chem. B* **2009**, *113*, 1381–1388.
(10) Li, C.; Wang, L.; Wei, M; Evans, D. G.; Duan, X. *J. Mater. Chem.* **2008**, *18*, 2666–2672.
(11) Iyi, N.; Ebina, Y.; Sasaki, T. *Langmuir* **2008**, *24*, 5591–5598.
(12) Liu, Z.; Ma, R.; Osada, M.; Iyi, N.; Ebina, Y.; Takada, K.; Sasaki, T. *J. Am. Chem. Soc.* **2006**, *128*, 4872–4880.
(13) Han, J. B.; Lu, J.; Wei, M.; Wang, Z. L.; Duan, X. *Chem. Commun.* **2008**, 5188–5190.
(14) Johnsen, R. E.; Wu, Q.; Sjåstad, A. O.; Vistad, Ø. B.; Krumeich, F.; Norby, P. *J. Phys. Chem. C* **2008**, *112*, 16733–16739.
(15) Li, L.; Ma, R.; Ebina, Y.; Fukuda, K.; Takada, K.; Sasaki, T. *J. Am. Chem. Soc.* **2007**, *129*, 8000–8007.
(16) Huang, S.; Peng, H.; Tjiu, W. W.; Yang, Z.; Zhu, H.; Tang, T.; Liu, T. *J. Phys. Chem. B* **2010**, *114*, 16766–16772.
(17) Bonnet, S.; Forano, C.; de Roy, A.; Besse, J. P.; Maillard, P.; Momenteau, M. *Chem. Mater.* **1996**, *8*, 1962–1968.
(18) Ukrainczyk, L.; Chibwe, M.; Pinnavaia, T. J.; Boyd, S. A. *J. Phys. Chem.* **1994**, *98*, 2668–2676.
(19) Barbosa, C. A. S.; Ferreira, A. M. D. C.; Constantino, V. R. L. *Eur. J. Inorg. Chem.* **2005**, 1577–1584.
(20) Halma, M.; de Freitas Castro, K. A. D.; Taviot-Guého, C.; Prévot, V.; Forano, C.; Wypych, F.; Nakagaki, S. *J. Catal.* **2008**, *257*, 233–243.
(21) Lang, K.; Bezdička, P.; Bourdelande, J. L.; Hernando, J.; Jirka, I.; Káfuňková, E.; Kovanda, F.; Kubát, P.; Mosinger, J.; Wagnerová, D. M. *Chem. Mater.* **2007**, *19*, 3822–3829.
(22) Káfuňková, E.; Taviot-Guého, C.; Bezdička, P.; Klementová, M.; Kovář, P.; Kubát, P.; Mosinger, J.; Pospíšil, M.; Lang, K. *Chem. Mater.* **2010**, *22*, 2481–2490.
(23) Demel, J.; Kubát, P.; Jirka, I.; Kovář, P.; Pospíšil, M.; Lang, K. *J. Phys. Chem. C* **2010**, *114*, 16321–16328.
(24) Lang, K.; Mosinger, J.; Wagnerová, D. M. *Coord. Chem. Rev.* **2004**, *248*, 321–350.
(25) Lang, K.; Kubát, P.; Mosinger, J.; Bujdák, J.; Hof, M.; Janda, P.; Sýkora, J.; Iyi, N. *Phys. Chem. Chem. Phys.* **2008**, *10*, 4429–4434.
(26) *JCPDS PDF-2 Database*, release 54; International Centre for Diffraction Data: Newtown Square, PA, 2004.
(27) Bubniak, G. A.; Schreiner, W. H.; Mattoso, N.; Wypych, F. *Langmuir* **2002**, *18*, 5967–5970.
(28) Wang, L.; Li, C.; Liu, M.; Evans, D. G.; Duan, X. *Chem. Commun.* **2007**, 123–125.
(29) Kubát, P.; Lang, K.; Procházková, K.; Anzenbacher, P. *Langmuir* **2003**, *19*, 422–428.

(30) Maiti, N. C.; Mazumdar, S.; Periasamy, N. *J. Phys. Chem. B* **1998**, *102*, 1528–1538.
(31) Mosinger, J.; Lang, K.; Plíštil, L.; Jesenská, S.; Hostomský, J.; Zelinger, Z.; Kubát, P. *Langmuir* **2010**, *26*, 10050–10056.
(32) Albery, W. J.; Bartlett, P. N.; Wilde, C. P.; Darwent, J. R. *J. Am. Chem. Soc.* **1985**, *107*, 1854–1858.
(33) Mosinger, J.; Jirsák, O.; Kubát, P.; Lang, K.; Mosinger, B. *J. Mater. Chem.* **2007**, *17*, 164–166.
(34) Levin, P. P.; Costa, S. M. B.; Ferreira, L. F. V.; Lopes, J. M.; Ribeiro, F. R. *J. Phys. Chem. B* **1997**, *101*, 1355–1357.
(35) Ogilby, P. R. *Chem. Soc. Rev.* **2010**, *39*, 3181–3209.
(36) Iu, K. K.; Thomas, J. K. *J. Photochem. Photobiol., A* **1993**, *71*, 55–60.
(37) Jockusch, S.; Sivaguru, J.; Turro, N. J.; Ramamurthy, V. *Photochem. Photobiol. Sci.* **2005**, *4*, 403–405.
(38) Cojocaru, B.; Laferrière, M.; Carbonell, E.; Parvulescu, V.; García, H.; Scaiano, J. C. *Langmuir* **2008**, *24*, 4478–4481.
(39) Pace, A.; Clennan, E. L. *J. Am. Chem. Soc.* **2002**, *124*, 11236–11237.